

# PCCP

Accepted Manuscript



This is an *Accepted Manuscript*, which has been through the Royal Society of Chemistry peer review process and has been accepted for publication.

*Accepted Manuscripts* are published online shortly after acceptance, before technical editing, formatting and proof reading. Using this free service, authors can make their results available to the community, in citable form, before we publish the edited article. We will replace this *Accepted Manuscript* with the edited and formatted *Advance Article* as soon as it is available.

You can find more information about *Accepted Manuscripts* in the [Information for Authors](#).

Please note that technical editing may introduce minor changes to the text and/or graphics, which may alter content. The journal's standard [Terms & Conditions](#) and the [Ethical guidelines](#) still apply. In no event shall the Royal Society of Chemistry be held responsible for any errors or omissions in this *Accepted Manuscript* or any consequences arising from the use of any information it contains.

## Boron-doped Graphene as Promising Anode for Na-ion Batteries

Cite this: DOI: 10.1039/x0xx00000x

Chen Ling,<sup>a\*</sup> and Fuminori Mizuno<sup>a</sup>

Received 00th January 2012,

Accepted 00th January 2012

DOI: 10.1039/x0xx00000x

www.rsc.org/

Na-ion battery has recently gained a lot of interest as a low-cost alternative to current Li-ion battery technology. Its feasibility strongly depends on the development of suitable electrode materials. In the present work we propose a novel anode candidate, boron-doped graphene, for Na-ion battery. Our first-principles calculations demonstrate the sodiation of boron-doped graphene well preserves its structural integrity. The 2D-BC<sub>3</sub> anode has the average sodiation voltage of 0.44 V in appropriate range to avoid the safety concerns caused by the formation of dendritic deposits. The capacity of 2D-BC<sub>3</sub> anode reaches ~2.04 times that of graphite anode in Li-ion battery and ~2.52 times that of hard carbon in Na-ion battery. The high electronic mobility and Na mobility on boron-doped graphene indicates it has a high potential to reach good rate performance. These suggest the promising potential of boron-doped graphene to serve as anode for rechargeable Na-ion battery.

### Introductions

Li-ion batteries (LIB) are the dominating power sources in the market of portable electronic devices. Yet its usage in large scale applications is still challenged by the high cost of lithium and possible supply risk.<sup>1</sup> An alternative battery based on sodium, the element with lower cost and higher abundance, has gained much interest recently.<sup>2,3</sup> Compared with lithium, the much larger ionic size and different reactivity of sodium strongly affect the electrochemical performance of electrode materials for sodium ion battery (NIB).<sup>4</sup> For instance, the capacity for the sodium insertion in graphite, the commercial anode in LIB, is too low for a practical NIB.<sup>3</sup> The primary choice of NIB anode at current moment is hard carbon, whose capacity (~300 mAh/g) is lower than the graphite anode in LIB.<sup>3</sup> Because of the safety concerns associated with its low sodiation voltage (less than 0.1 V vs Na/Na<sup>+</sup>), hard carbon may only be suitable in the lab-test. Alloy

anodes such as Sn and Sb exhibited good capacity for the sodiation.<sup>5</sup> But the pulverization caused by the large volume expansion potentially damages their long cycling performance.<sup>6</sup> Intercalation-type materials such as lithium titanate and sodium titanate have been reported with voltages for Na insertion as low as 0.3 V vs Na/Na<sup>+</sup>.<sup>7</sup> However, the energy densities of these materials are limited by the low capacities, and their cyclabilities challenge real applications.

To date, the sought of NIB anode candidate is still highly demanded to meet the following requests: (1) high energy density; (2) appropriate sodiation voltage to avoid the dendrite formation; (3) good cyclability and (4) good rate capability.<sup>3</sup> In this Communication, we propose a new candidate, boron doped graphene, as promising NIB anode. Equipped with first-principles calculations we have systematically investigated the capacity, sodiation voltage, structural deformation and rate capability of boron doped graphene. The results demonstrate this material has encouraging potential to achieve high energy density with appropriate voltages to avoid safety issues raised by sodium plating and dendrite formation, good rate capability and stable cyclability. These make boron-doped graphene promising anode candidate for future rechargeable Na-ion batteries.

### Results and discussions

Since the discovery of graphene in 2004, the emerging 2D materials have attracted great interest because of their fascinating physical and chemical properties. The adsorption of Li on graphene and its analogues, including monolayer and few-layer graphene,<sup>8</sup> chemical doped graphene,<sup>9</sup> graphyne,<sup>10</sup> and silicene,<sup>11</sup> has been extensively studied. On the contrary, the knowledge about the adsorption of Na on graphene sheet is very limited. Our study begins with calculating the adsorption energy of Na in pristine graphene. The adsorption energies at dilute Na loading are positive (Figure S1), with the lowest value of +0.50 eV at the hollow site. It indicates that Na is energetically unstable to adsorb on pristine graphene even at low concentrations.

Therefore the pristine graphene cannot be used directly as the active material for NIB anode. Note that in some previous theoretical investigations the adsorption energy of Na on pristine graphene was negative.<sup>12, 13</sup> This discrepancy can be attributed to the different Na reference states. In the application of battery electrode, the natural and correct reference state should be the stable metallic phase of Na, instead of a neutral Na atom in the gaseous phase.

An effective way to tune the property of graphene is chemical doping.<sup>14</sup> For this purpose we turn our focus to nitrogen-doped and boron-doped graphene, both of which keep the planar structure of graphene without too much structural deformation.<sup>9</sup> The adsorption energy on N-doped graphene (2D-NC<sub>31</sub>) is more positive (+0.88 eV), indicating that the doping of electron-abundant nitrogen makes the adsorption more energetically unfavorable. On the other hand, boron doping greatly decreases the adsorption energy. The adsorption energy of single Na on 2D-BC<sub>31</sub> is -0.79 eV, making it an interesting candidate for our further investigations. The adsorption of the second Na on 2D-BC<sub>31</sub>, however, is energetically unstable. The capacity of BC<sub>31</sub> is therefore limited to Na<sub>1</sub>(BC<sub>31</sub>), about 70 mAh/g. It is necessary to increase boron content in order to improve its capacity.

The feasibility of using boron doped graphene with higher boron contents as NIB anode is then investigated using two B-doping graphene sheets, 2D-B<sub>0.5</sub>C<sub>3.5</sub> and 2D-BC<sub>3</sub> (Figure 1), as examples. The capacity, the voltage for the sodiation, the structural deformation caused by the sodiation and the rate capability are explored systematically and discussed in details.

The maximum capacity for the sodiation of boron-doped graphene can be estimated by calculating the formation energy of Na<sub>x</sub>(B<sub>y</sub>C<sub>4-y</sub>) as

$$E_f = E_{NaBC} - E_{BC} - x\mu_{Na} \quad (1)$$

Here  $E_{NaBC}$ ,  $E_{BC}$  and  $\mu_{Na}$  is the total energy of Na<sub>x</sub>(B<sub>y</sub>C<sub>4-y</sub>), the total energy of B<sub>y</sub>C<sub>4-y</sub>, and the chemical potential of the reference metallic Na, respectively. Under this definition, the maximum capacity corresponds to the concentration at which the slope of the formation energy curve becomes positive (see Supporting Information). The sodiation curves are shown in Figure 1c and 1d for 2D-B<sub>0.5</sub>C<sub>3.5</sub> and 2D-BC<sub>3</sub>, respectively. For both materials, we have calculated the adsorption on single side (single-side adsorption) and on both sides (double-side adsorption) of the graphene sheet. For 2D-B<sub>0.5</sub>C<sub>3.5</sub>, the maximum Na concentration is predicted to be Na<sub>0.75</sub>(B<sub>0.5</sub>C<sub>3.5</sub>) and Na<sub>0.625</sub>(B<sub>0.5</sub>C<sub>3.5</sub>) for double-side and single-side adsorption, respectively. For 2D-BC<sub>3</sub>, it becomes Na<sub>1.33</sub>(BC<sub>3</sub>) and Na<sub>1.125</sub>(BC<sub>3</sub>) for double-side and single-side adsorption, respectively. In all cases the maximum concentration is in excess of one Na per doped boron. If the concentration is translated to the capacity, it corresponds to a capacity of 423(353) and 762(648) mAh/g for the double(single)-side adsorption on 2D-B<sub>0.5</sub>C<sub>3.5</sub> and 2D-BC<sub>3</sub>, respectively. The maximum value here is about twice of the capacity of graphite anode (370 mAh/g) in LIB.

The calculated sodiation curve also enables the prediction of the voltages for the electrochemical adsorption of Na. With the assumption that the contribution of the entropy is neglected, the voltage is obtained as<sup>15</sup>

$$V = -(E_{a,x_2} - E_{a,x_1} - (x_2 - x_1)\mu_{Na}) / ((x_2 - x_1)e) \quad (2)$$

Here  $x_1$  and  $x_2$  are two adjacent points along the sodiation curve. The voltages are shown in Figure 1e-f. The average voltages are

0.61 (0.57) and 0.44 (0.22) V for the double(single)-side adsorption on 2D-B<sub>0.5</sub>C<sub>3.5</sub> and 2D-BC<sub>3</sub>, respectively. These numbers averaged in the whole capacity range.

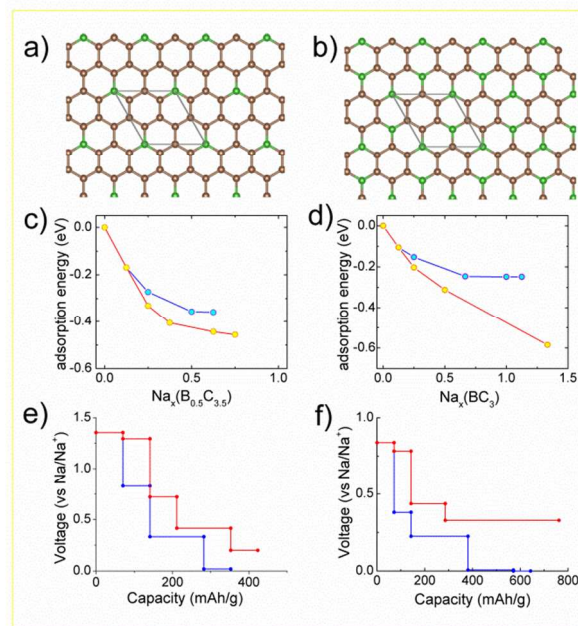


**Fig. 1** (a). Structure of 2D-B<sub>0.5</sub>C<sub>3.5</sub>. (b) Structure of 2D-BC<sub>3</sub>. The unit cells are marked with gray rhombus. (c) Formation energy of sodiated 2D-B<sub>0.5</sub>C<sub>3.5</sub>. (d) Formation energy of sodiated 2D-BC<sub>3</sub>. (e) Voltages for the sodiation of 2D-B<sub>0.5</sub>C<sub>3.5</sub>. (f) Voltage for the sodiation of 2D-BC<sub>3</sub>. In (c-f), the blue color shows the adsorption on one-side of the 2D-layer, while the red color shows the adsorption on both sides of the 2D-layer.

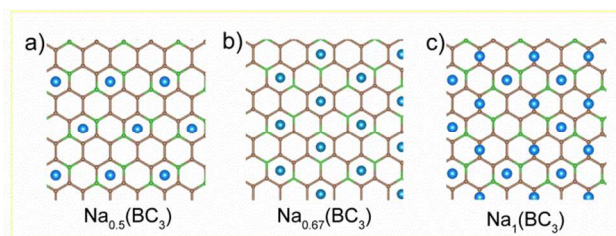


**Fig. 2** Structures of sodiated 2D-Na<sub>x</sub>BC<sub>3</sub>. (a) Na<sub>0.5</sub>(BC<sub>3</sub>); (b) Na<sub>0.67</sub>(BC<sub>3</sub>); (c) Na(BC<sub>3</sub>). All the structures are taken from the ground states for single-side adsorption.

In order to gather more insight about the sodiation process, the structures of sodiated phase are analyzed. Figure 2 shows the single-side adsorption on 2D-BC<sub>3</sub> as an example for our discussion. Sodium preferably occupies the hollow site at concentrations lower than Na<sub>0.67</sub>(BC<sub>3</sub>). In Na<sub>0.5</sub>(BC<sub>3</sub>) all Na are ordered with the smallest distance 2a (a is the distance between two nearest hollow sites), while in Na<sub>0.67</sub>(BC<sub>3</sub>) all Na are ordered with the smallest distance  $\sqrt{3}a$ . We have also carried out the calculations for configurations with Na ions at adjacent hollow sites and found their relative energies are at least 0.1 eV higher.

It suggests strong repulsion between nearest Na ions prevents the occupation of adjacent sites at low loadings (less than  $\text{Na}_{0.67}(\text{BC}_3)$ ). Continuous adsorption beyond  $\text{Na}_{0.67}(\text{BC}_3)$  leads to the occupation of neighbored hollow sites. To minimize the repulsion, those adjacent Na ions are displaced against each other after relaxation. It can be seen in Figure 2c for  $\text{Na}_1(\text{BC}_3)$ , in which half of adsorbed Na ions are displaced from the hollow site to the bridge site after DFT relaxation.

**Table 1.** Bond distance ( $d$ ) and the vertical displacement of atoms ( $z$ ) in sodiated 2D- $\text{Na}_x(\text{BC}_3)$ . For  $\text{Na}_1(\text{BC}_3)$ , two values of Na bond distances are shown for sodium occupying bridge site/hollow site. The negative value of the vertical displacement indicate the displacement is outward the adsorbed sodium, while the positive value indicate the displacement is toward sodium. All values are shown with the unit Å.

	$\text{Na}_0$	$\text{Na}_{0.5}$	$\text{Na}_{0.67}$	$\text{Na}_1$
$d(\text{B-C})$	1.56	1.56	1.55	1.55
$d(\text{C-C})$	1.42	1.43	1.43	1.43
$d(\text{Na-C})$		2.60	2.65	2.55/2.70
$d(\text{Na-B})$		2.61	2.68	3.13/2.71
$z_{\text{B}}$	0.00	-0.02	-0.02	-0.05
$z_{\text{C}}$	0.00	0.01	0.01	0.03
$z_{\text{Na}}$		2.11	2.20	2.42/2.25

To analyze the structure deformation caused by the sodiation following the process in Figure 2, the boron-carbon and carbon-carbon bond lengths are first measured to evaluate the integrity of the graphene sheet. The distances of boron-carbon and carbon-carbon bond only vary by  $\sim 0.01$  Å after the sodiation (Table 1), suggesting the structural integrity of the graphene sheet is well-maintained. This could be beneficial for the cycling of the electrode.<sup>16</sup> The characteristic structural deformation is the displacement of lattice atom along vertical directions. For sodium concentration lower than  $\text{Na}_{0.67}(\text{BC}_3)$ , boron and carbon atoms that are neighbored to sodium only experience very small displacements ( $\leq 0.02$  Å). It suggests that at low sodium loadings the structure deformation is actually negligible. The displacement becomes more noticeable for  $\text{Na}_1(\text{BC}_3)$ , at which half of adsorbed sodium ions are displaced from the hollow sites to the bridge sites. This change of adsorption site disturbs the neighbored atoms by pushing (attracting) boron (carbon) away from the planar plane. The distance between boron (carbon) and sodium ion at the bridge site also becomes significantly longer (shorter). This stronger structural deformation may potentially damage the cycling performance of the electrode. It is thus important to keep the sodiation level below  $\text{Na}_{0.67}(\text{BC}_3)$  for the sodiation of 2D- $\text{BC}_3$  in order to achieve better cycling performance.

Following these results, we explain the sodiation of boron doped graphene as a competition between the chemical bonding of Na and graphene layer, and the repulsion between Na ions. Let's first explain the chemical bonding effect. Pristine graphene forms through  $sp^2$  bonding between carbon atoms, in which the  $\pi$  orbitals form a passivative layer for the bonding with other ions.<sup>17</sup> Boron in the atomic graphene layer acts as p-type dopant.<sup>9</sup> Boron substitution generates an electron deficient matrix, in

which the electrons in the boron-carbon bond are attracted towards the more electronegative carbon atom (Figure 3a). Na bound to graphene, on the other hand, acts as n-type dopant.<sup>9</sup> Using Bader analysis we find that each Na atom donates a charge of  $\sim 0.9e$  to the graphene layer, indicating Na is almost fully ionized. The donated electron saturates the electron-deficient boron-carbon bond (Figure 3b). It results in a chemical bonding between B-doped graphene and  $\text{Na}^+$  ions, which shifts the adsorption energy from positive to negative values. This chemical bonding dominates the adsorption at low Na loadings. As a result, the voltages for the sodiation at low concentrations are quite considerable, which is beneficial to eliminate the safety concerns caused by sodium plating at this stage.

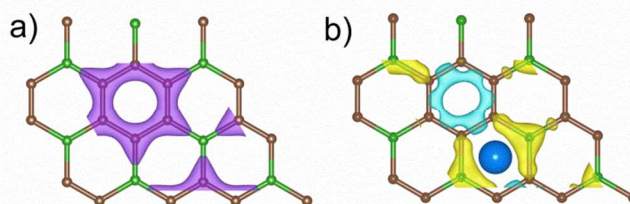


**Fig. 3** (a) Electron density on 2D- $\text{BC}_3$  layer. The purple color shows the isosurface at  $0.1 \text{ bohr}^{-3}$ . Boron is not covered by the isosurface, indicating the electron density is deficient around boron site. (b) Variation of electron density after the adsorption of Na on 2D- $\text{BC}_3$  layer (double side adsorption at concentration  $\text{Na}(\text{BC}_3)$ ). The yellow color shows the isosurface at  $+0.008 \text{ bohr}^{-3}$ , the cyan color shows the isosurface at  $-0.008 \text{ bohr}^{-3}$ .

At high Na loading, the chemical bonding is balanced by the repulsion between ionized  $\text{Na}^+$ . By analyzing the relaxed structure we find that the distance of nearest Na-Na pairs should be at least  $3.26$  Å. This value is much higher than the distance between two adjacent hollow sites,  $\sim 2.5$  Å. To minimize the repulsion, adjacent Na ions have to be displaced from the center of the hollow site. It could even result in a change of the adsorption site. At  $\text{Na}_1(\text{BC}_3)$ , half of Na are displaced from the hollow sites to the bridge sites. This displacement and associated large structural deformation greatly decrease the adsorption energy. The sodiation from  $\text{Na}_{0.67}(\text{BC}_3)$  to  $\text{Na}_1(\text{BC}_3)$  happens at voltages less than  $0.02$  V (single-side adsorption, Figure 1f). It indicates that the sodiation at high loading is actually close to the direct plating of sodium. Thus we conclude that it is necessary to keep the sodiation level below  $\text{Na}_{0.67}(\text{BC}_3)$  in order to avoid the potential structure destruction at higher sodium loading and to minimize the safety issue caused by possible sodium plating. If the sodiation is terminated before the voltage becomes lower than  $0.1$  V, the average voltage becomes  $0.37$  ( $0.71$ ) V with a truncated capacity  $381$  ( $282$ ) mAh/g for the single-side adsorption on 2D- $\text{BC}_3$  ( $\text{B}_{0.5}\text{C}_{3.5}$ ). For double-side adsorption on 2D- $\text{BC}_3$  ( $\text{B}_{0.5}\text{C}_{3.5}$ ), the average voltage becomes  $0.44$  ( $0.61$ ) V and the truncated capacity is  $762$  ( $423$ ) mAg/h. Note the voltage for the double-side adsorption is always higher than  $0.1$  V. Thus the capacity and the average voltage for the double-side adsorption are not affected by the truncation.

On the basis of the above analysis, we argue that the 2D- $\text{BC}_3$  actually provides the best choice in terms of energy density and cyclability. Let us consider a composition  $\text{BC}_x$ . Compared to

pristine graphene, this material contains one electron deficiency per  $\text{BC}_x$  unit. In order to saturate this deficiency, one Na can be attracted to the surface, giving a capacity one Na per  $\text{BC}_x$  unit. From our results we can say the real adsorption is more complicated than this simple estimation, because the maximum amount of adsorbed Na is actually in excess of one Na per boron. Therefore, smaller values of  $x$  are beneficial to provide higher capacity. On the other hand, the adsorption of Na is also limited by the repulsion between nearest  $\text{Na}^+$ . The displacement of Na ions at high loading and the associated structural deformation would potentially damage the cycling performance of the anode. The adsorption of Na at low sodiation voltage is also not desirable for safety concerns. The highest Na loading without any nearest Na-Na pairs is  $\text{Na}_{0.167(1+x)}(\text{BC}_x)$  for single-side sodiation, and  $\text{Na}_{0.333(1+x)}(\text{BC}_x)$  for double-side sodiation. Our calculated results show that the highest Na loading has already been achieved for 2D- $\text{BC}_3$ , which has a capacity of  $\text{Na}_{1.333}(\text{BC}_3)$  for double-side sodiation, and  $\text{Na}_{1.125}\text{BC}_3$  for single-side sodiation. It is no longer necessary to further increase B concentration beyond  $\text{BC}_3$  for even higher capacities. Note that in fact 2D- $\text{BC}_3$  is also the highest boron doping level that has been achieved experimentally.<sup>18</sup>

A possible concern that probably limits the usage of 2D-boron doped graphene as Na battery anode is the formation of solid-electrolyte-interface (SEI) layer, which could potentially block the adsorption and transportation of  $\text{Na}^+$  ions. If the sodiation voltage of the anode outside the electrochemical window of the electrolyte, the electron from the external circuit is preferably transferred to the conduction band of the electrolyte, which reduces the electrolyte (usually anion) and forms SEI layer.<sup>19</sup> The conduction band minimum varies in different electrolytes from 0.9 V to 1.3 V vs  $\text{Li}/\text{Li}^+$ , which is around 0.6-1.0 vs  $\text{Na}/\text{Na}^+$ .<sup>19</sup> It can be seen that the average sodiation voltage (0.44 V vs  $\text{Na}/\text{Na}^+$ ) of the proposed candidate, 2D- $\text{BC}_3$ , is indeed only slightly lower than this limitation. If the sodiation is limited before it reaches the full capacity, the average sodiation voltage can be further adjusted. For 2D- $\text{BC}_3$ , the average sodiation voltage is 0.62 V vs  $\text{Na}/\text{Na}^+$  if the sodiation is limited to  $\text{Na}_{0.5}(\text{BC}_3)$ . Although such limited sodiation sacrifices the capacity to 286 mAh/g, this value already locates within the electrochemical window of some ionic liquid electrolytes.<sup>19</sup> It is therefore of great interest to analyze the performance of 2D- $\text{BC}_3$  by adjusting the voltage window in the test.

Challenges raised by possible SEI formation on the surface can also be tackled with material design and/or interfacial design.<sup>20</sup> A strategy here is to use multilayer boron-doped graphene. For multilayer graphene, the charge carrier  $\text{Na}^+$  can either be intercalated inside layers, or adsorbed on the surface. To explore the performance of stacked boron-doped graphene as Na-ion battery anode, we explicitly calculate the intercalation and adsorption of Na in bi-layer and tri-layer  $\text{BC}_3$ , as well as the intercalation in bulk 3D- $\text{BC}_3$  (see ESI for details). The average voltage for Na intercalation and adsorption lie around 1.1-1.3 V and 0.4-0.5 V, respectively (Fig. 4a). The higher voltage for the intercalation is a result of the stronger bonding strength because the intercalated Na interacts with two graphene layers and the adsorbed Na only reacts with one layer. Interestingly, neither the intercalation voltage nor the adsorption voltage is significantly affected by the number of layers. This observation is in contrast to the lithiation of layered graphene, for which bilayer graphene had the highest voltage.<sup>8</sup> Such discrepancy can be

explained by the bonding characteristics between graphene and the adsorbates (Li or Na). For the lithiation of pristine graphene, the exterior layer forms more ionic bonds with Li. Thus the insertion in bilayer graphene, which only has two exterior layers, shows the strongest binding strength.<sup>8</sup> For boron-doped graphene, the electronic hole greatly enhances the electron transfer from the adsorbed Na to the substrate layer (Fig. 3b). In this case  $\text{Na}^+$  forms completely ionic bond with either exterior or interior layer, which eliminates the difference between bilayer and other stacked boron-doped graphene.

While stacking graphene layers is able to increase the voltage to avoid SEI formation, it also sacrifices the sodiation capacity. Figure 4b shows the average sodiation voltage and capacity for different layered  $\text{BC}_3$  anodes. Theoretically, for  $n$ -layer  $\text{BC}_3$  anode, it is able to intercalate  $0.67(n-1)$   $\text{Na}^+$  and adsorb  $1.33$   $\text{Na}^+$  on both sides. Therefore the total capacity is  $0.67(n+1)$  per  $(\text{BC}_3)_n$ . This value is at the maximum for monolayer  $\text{BC}_3$  ( $\text{Na}_{1.33}\text{BC}_3$ ) and converges to  $\text{Li}_{0.67}(\text{BC}_3)$  for 3D  $\text{BC}_3$  anode, which is the almost same as the graphite anode with a capacity of  $\text{LiC}_6$ .<sup>8</sup> High voltage and low capacity are both negative for the anode energy density. It is therefore important to use few layer boron-doped graphene in order to provide desirable energy density. Further experimental effort is necessary to seek the best performance for the stacked  $\text{BC}_3$  anodes.

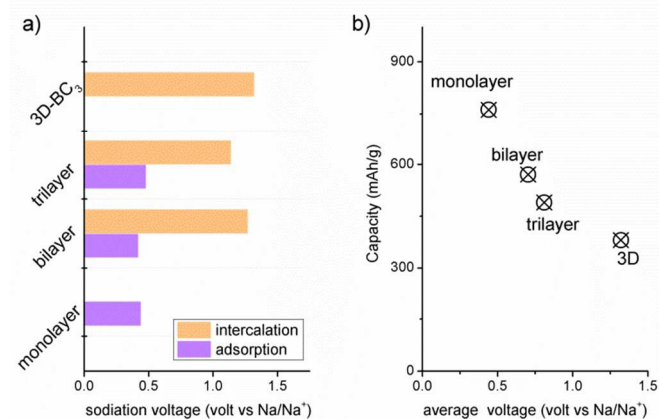


**Fig. 4** Stacked  $\text{BC}_3$  as Na-ion battery anode. (a) The calculated voltage for Na intercalation in and adsorption on few layer  $\text{BC}_3$ . (b) The average voltage and capacity of few layer  $\text{BC}_3$ .

Our final target is to evaluate the rate performance of B-doped graphene as NIB anode. The rate capability of an electrode material is limited by the kinetics of the electron transport as well as the cationic transport. Pristine graphene has exceptional carrier mobilities in excess of  $200,000 \text{ cm}^2/(\text{V}^3 \text{ s}^3)$ .<sup>21</sup> Compared with the pristine zero-band gap graphene, the doping of boron opens the band gap and makes the boron-doped graphene a narrow bandgap semiconductor (Figure 5a). After Na adsorption, the band gap vanishes and the whole compound becomes metallic (Figure 5b). It indicates the electron mobility on this material can be very fast, which should not limit the adsorption kinetics.

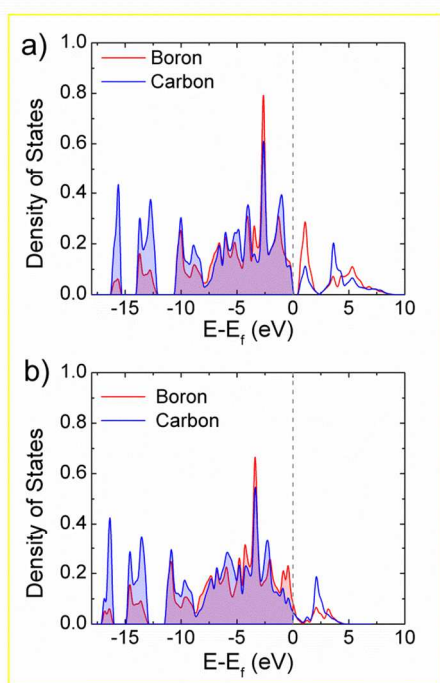


**Fig. 5** Electronic structure of boron-doped graphene. (a) pristine 2D-BC<sub>3</sub> and (b) 2D-Na(BC<sub>3</sub>).

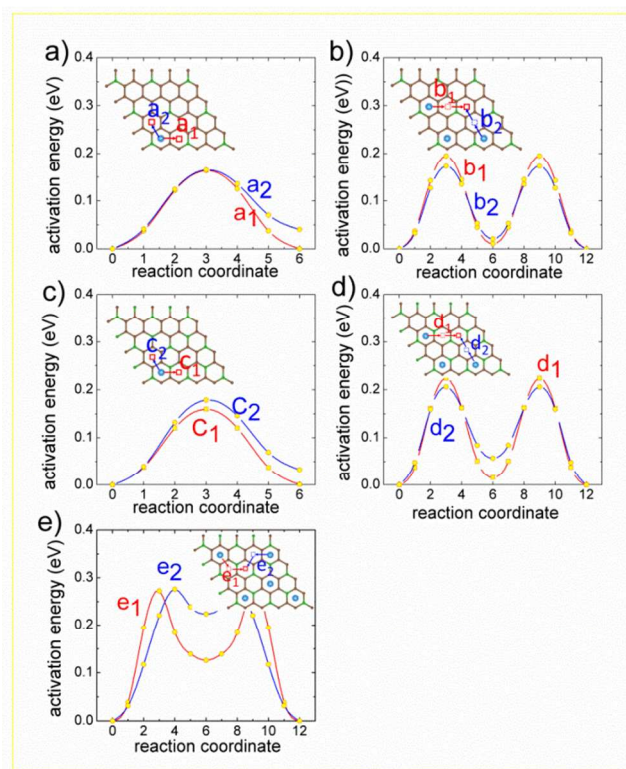


**Fig. 6** Diffusion of Na on boron-doped graphene layer at different Na concentrations. (a) at Na<sub>ε</sub>(B<sub>0.5</sub>C<sub>3.5</sub>); (b) at Na<sub>0.5-ε</sub>(B<sub>0.5</sub>C<sub>3.5</sub>); (c) at Na<sub>ε</sub>(BC<sub>3</sub>); (d) at Na<sub>1-ε</sub>(BC<sub>3</sub>); and (e) at Na<sub>1.33-ε</sub>(BC<sub>3</sub>). Here ε denotes a small change of the concentration.

To assess the kinetics for the transport of Na ions, calculations about the activation energy barriers for the diffusion of Na<sup>+</sup> are carried out at different Na loadings. The results are summarized in Figure 6. If the diffusion path does not involve formation of adjacent Na<sup>+</sup>, the activation energy barrier is in the range of 0.16–0.22 eV. This type of diffusion dominates at low Na loading (Figure 6a–6d). At high Na loading such as Na<sub>1.33</sub>(BC<sub>3</sub>), the diffusion path contains an intermediate state with Na<sup>+</sup> occupying adjacent sites, which generates large repulsion and destabilizes the intermediate state by 0.1–0.2 eV. In this case the activation energy barrier is increased to 0.27–0.28 eV (Figure 6e). Interestingly, these values are similar to Na diffusion on pristine graphene surface,<sup>13</sup> and do not show strong dependence on the local environment, indicating the diffusion of Na is not trapped at any specific site. All these values are comparable to or even lower than the diffusion barrier of Li<sup>+</sup> in typical LIB electrodes.<sup>22</sup> We note the barrier for Na diffusion is lower than that of Li diffusion on boron-doped graphene at high Li concentration, ~0.40 eV.<sup>9</sup> It indicates that B-doped graphene can have unique advantages as high rate NIB anode.

## Conclusions

To summarize our results, in this Communication a promising material, boron-doped graphene, is proposed as the anode candidate for Na-ion batteries. The maximum capacity of boron-doped graphene can reach 762 mAh/g with an average sodiation voltage 0.44 V for the adsorption of Na on both sides of 2D-BC<sub>3</sub>. This value is about 2.06 times that of graphite anode in Li-ion battery (~370 mAh/g), and 2.54 times that of hard carbon anode in Na-ion battery (~300 mAh/g). The average sodiation voltage of 0.44 V is in the appropriate range to avoid the safety concerns caused by the formation of dendritic deposits. The sodiation well preserves the structural integrity of 2D-nanosheet with negligible displacement of the lattice atoms, which is beneficial for a good cyclability. The high electronic mobility and Na mobility indicate good rate capability of this promising anode. These fascinating properties suggest boron-doped graphene is a promising anode candidate for NIB. With progressively advances on the synthesis of boron-doped graphene, we believe that it can indeed become a practical choice of anode material in NIB.

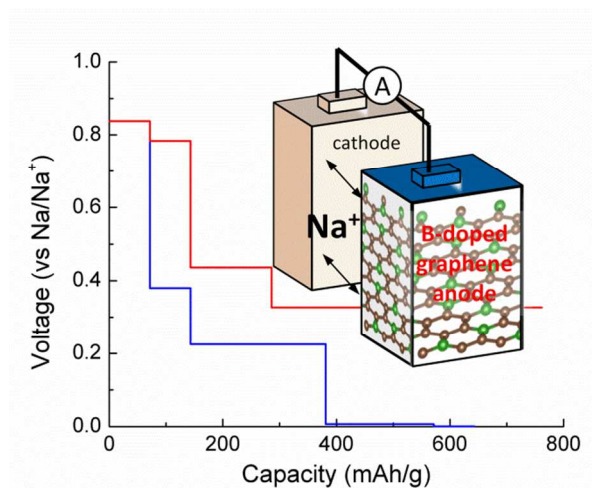
## Notes and references

<sup>a</sup> Toyota Research Institute of North America, 1555 Woodridge Ave, Ann Arbor, Michigan, USA, 48105. Email: chen.ling@tema.toyota.com  
Electronic Supplementary Information (ESI) available: Computational details; Method to estimate of the maximum amount of adsorbed Na; Energy density of different anode materials.details of any supplementary information available should be included here. See DOI: 10.1039/c000000x/

- 1 M. Armand and J.-M. Tarascon, *Nature*, 2008, **451**, 652
- 2 V. Palomares, P. Serras, I. Villaluenga, K. B. Hueso, J. Carretero-Gonzalez and T. Rojo, *Energy Environ. Sci.*, 2012, **5**, 5884; S. Kim, D. Seo, X. Ma, G. Ceder and K. Kang, *Adv. Energy Mater.*, 2012, **2**, ; B. L. Ellis and L. F. Nazar, *Current Opinion in Solid State Mater. Sci.*, 2012, **16**, 168

- 3 M. D. Slater, D. Kim, E. Lee and C. S. Johnson, *Adv. Funct. Mater.*, 2013, **23**, 947
- 4 S. P. Ong, V. L. Chevrier, G. Hautier, A. Jain, C. Moore, S. Kim, X. Ma and G. Ceder, *Energy Environ. Sci.*, 2011, **4**, 3680; S. Kim, X. Ma, S. P. Ong and G. Ceder, *Phys. Chem. Chem. Phys.*, 2012, **14**, 15571; S. Y. Hong, Y. Kim, Y. Park, A. Choi, N.-S. Choi and K. T. Lee, *Energy Environ. Sci.*, 2013, **6**, 2067; C. Ling, J. Chen and F. Mizuno, *J. Phys. Chem. C*, 2013, **117**, 21158
- 5 J. Qian, Y. Chen, L. Wu, Y. Cao, X. Ai and H. Yang, *Chem. Commun.*, 2012, **48**, 7070; A. Darwiche, C. Marino, M. T. Sougrati, B. Fraisse, L. Stievano and L. Monconduit, *J. Am. Chem. Soc.*, 2012, **134**, 20805
- 6 V. L. Chevrier and G. Ceder, *J. Electrochem. Soc.*, 2011, **158**, A1011
- 7 P. Senguttuvan, G. Rousse, M. E. Arroyo de Dompablo, H. Vezin, J.-M. Tarascon and M. R. Palacin, *J. Am. Chem. Soc.*, 2013, **135**, 3897; Y. Sun, L. Zhao, H. Pan, X. Lu, L. Gu, Y. Hu, H. Li, M. Armand, Y. Ikuhara, L. Chen and X. Huang, *Nature Commun.*, 2013, **4**, 1870; P. Senguttuvan, G. Rossue, V. Seznec, J.-M. Tarascon and M. R. Palacin, *Chem. Mater.*, 2011, **23**, 4109
- 8 E. Lee and K. A. Persson, *Nano Lett.*, 2012, **12**, 4624
- 9 Y. Liu, V. I. Artyukhov, M. Liu, A. R. Harutyunyan and B. I. Yakobson, *J. Phys. Chem. Lett.*, 2013, **4**, 1737
- 10 H. J. Hwang, J. Koo, M. Park, N. Park, Y. Kwon and H. Lee, *J. Phys. Chem. C*, 2013, **117**, 6919
- 11 G. A. Tritsarlis, E. Kaxiras, S. Meng and E. Wang, *Nano Lett.*, 2013, **13**, 2258
- 12 K. T. Chan, J. B. Neaton and M. L. Cohen, *Phys. Rev. B*, 2008, **77**, 235430; T. O. Wehling, M. I. Katsnelson and A. I. Lichtenstein, *Phys. Rev. B*, 2009, **80**, ; L. Qiao, C. Q. Qu, H. Z. Zhang, S. S. Yu, X. Y. Hu, X. M. Zhang, D. M. Bi, Q. Jiang and W. T. Zheng, *Diamond Related Mater.*, 2010, **19**, ; X. Liu, C. Z. Wang, Y. X. Yao, W. C. Lu, M. Hupalo, M. C. Tringides and K. M. Ho, *Phys. Rev. B*, 2011, **83**, 235411
- 13 K. Nakada and A. Ishii, *Solid State Commun.*, 2011, **151**, 13
- 14 W. Z., R. W., L. Xu, F. Li and H. Cheng, *ACS Nano*, 2011, **5**, 5463; H. Sheng, D. Wu, S. Li, F. Zhang and X. Feng, *Small*, 2013, **9**, 1173
- 15 C. Ling, D. Banerjee, W. Song, M. Zhang and M. Matsui, *J. Mater. Chem.*, 2012, **22**, 13517; C. Ling and F. Mizuno, *Chem. Mater.*, 2012, **24**, 3943; C. Ling and F. Mizuno, *Chem. Mater.*, 2013, 3062
- 16 H. Kim, I. Park, S. Lee, H. Kim, K.-Y. Park, Y.-U. Park, H. Kim, J. Kim, H.-D. Lim, W.-S. Yoon and K. Kang, *Chem. Mater.*, 2013,
- 17 J. E. Johns and M. C. Hersam, *Accounts Chem. Res.*, 2013, **1**, 77
- 18 H. Yanagisawa, T. Tanaka, Y. Ishida, M. Matsue, E. Rokuta, S. Otani and C. Oshima, *Phys. Rev. Lett.*, 2004, **93**,
- 19 J. B. Goodenough and Y. Kim, *Chem. Mater.*, 2010, **22**, 587
- 20 Y. Sun, Q. Wu and G. Shi, *Energy Environ. Sci.*, 2011, **4**, 1113
- 21 S. V. Morozov, K. S. Novoselov, M. I. Katsnelson, F. Schedin, D. C. Elias, J. A. Jaszczak and A. K. Geim, *Phys. Rev. Lett.*, 2008, **100**, 016602
- 22 Y. S. Meng and M. E. A.-d. Dompablo, *Energy Environ. Sci.*, 2009, **2**, 589

## Graphic Abstract



We propose boron-doped graphene as Na-ion battery anode with potential to greatly enhance the energy density and rate capability.